Microelectronic Engineering 143 (2015) 11–14

Contents lists available at ScienceDirect

Microelectronic Engineering

journal homepage: www.elsevier.com/locate/mee

Nanofabrication of air-spaced field-plate gates with ultra-short footprint

Jinhai Shao [a], Jianpeng Liu [a], Junjie Li [a], Sichao Zhang [a], Bing-Rui Lu [a], W. Lu [b], Yifang Chen [a,*]

[a] State Key Lab of ASIC and System, School of Information Science and Engineering, Fudan University, Shanghai 200433, China
[b] Department of Electrical and Computer Engineering, Ohio State University, Columbus, OH 43210, USA

ARTICLE INFO

Article history:
Received 24 October 2014
Received in revised form 25 December 2014
Accepted 19 January 2015
Available online 28 January 2015

Keyword:
Air-spaced field-plate gate
Electron beam lithography
Reactive ion etch
SiNx

ABSTRACT

This paper reports our recent work on nanofabrication of air-spaced field-plate (ASFP) gates with ultra-short foot-print using one step electron beam lithography (EBL) combined with reactive ion etch (RIE) for which are suitable for GaN based high electron mobility transistors (HEMTs). Electron beam lithography on a tri-layer stack with PMMA350K/PMMA100K/Al/UVIII is carried out to form the required profile in resist. A low damage RIE dry-etch process is developed to create two different kinds of shapes in the 100 nm SiNx layer which serves as a footprint definition and mechanical support to the field-plate. The process enables us to fabricate air spaced field-plates with 60 nm foot-print and 50 nm air gap. Its advantages over traditional field-plates as well as T shape gate are discussed.

1. Introduction

High electron mobility transistors (HEMTs) are the key components in communication and imaging applications in both microwave and terahertz [1]. AlGaN/GaN heterojunctions based on broad band GaN have unique advantages of high carrier density, high mobility and deep confining well, being widely applied in HEMTs with high power. However, the uneven charge accumulated in the heterojunction causes a static field peak near the drain, leading to low breakdown voltage. To suppress the peak field, a broad field-plate gate is usually implemented directly on the SiNx passivation layer at the cost of scarifying high frequency performance because of the induced parasitic capacitance [2]. To solve this problem, we have developed an air-spaced field-plate gate (ASFP gate) with significantly reduced contact area, which appears like a broad head T shape gate as conceptually shown in Fig. 1c. In this configuration, the air space underneath the field-gate greatly reduces the parasitic capacitance [3]; meanwhile, the short space still enables the field-plate to suppress the peak field near the drain [4]. It is therefore expected that with such an ASFP gate, both high frequency and high power can be achieved in GaN based HEMTs. To the best of our knowledge, air-spaced field plates particularly on GaN-HEMTs have not been reported so far.

It is realized that when the aspect ratio (headwidth/footprint) is increased, its mechanical reliability becomes unstable [5–8]. The main focus of this paper is to design the layer structure in resists based on the processing study of EBL with the mechanical reliability taking into consideration, and fabricate the ASFP gates using multilayer resists stacks and SiNx layer by combing EBL with RIE technique. The advantages of ASFP gates lie in the reduced parasitic capacitance, reduced gate resistance and increased breakdown voltage comparing with traditional field plates. It is believed that the developed fabrication technique is hopefully applicable for high frequency and high power GaN based HEMTs.

2. Experiments

Fig. 1 shows the process flow for the fabrication of the ASFP gate. First, a 100 nm thick SiNx is deposited on the substrate using low pressure chemical vapor deposition (LPCVD). The SiNx layer is used to improve the definition of the foot and also acts as a mechanical supporting layer. Then, a 60 nm thick PMMA (350K) and 150 nm PMMA (100K) are spin coated onto the substrate, followed by an oven bake at 180 °C for one hour for each layer. After that, a 10 nm thick aluminum is deposited using a thermal heating evaporator. In the end, a 500 nm thick UVIII, which is chemically amplified resist (CAR) delivered by Shipley Ltd., is spin coated and subsequently baked on a hot plate at 130 °C for 1 min. As a positive tone CAR, UVIII is widely used for electron beam lithography due to its high sensitive capability and nanoscale capability [9]. The thin aluminum layer between the PMMA bilayer and UVIII layer facilitates the removal of the UVIII scum caused by heavy dose of e-beam exposure [10]. Electron beam exposure is carried out by a JEOL 6300FS at 100 keV with a typical beam current of 500 pA and an 8 nm beam-spot size. A dose between 40 and 50 $\mu C/cm^2$ is used to pattern the head of the broad field-plate gate. There are at least two folds of advantages with the UVIII being used

* Corresponding author.
E-mail address: yifangchen@fudan.edu.cn (Y. Chen).

http://dx.doi.org/10.1016/j.mee.2015.01.019

for the plate. One is that the writing time is shortened by a factor of ~6 comparing with when a copolymer layer is applied for the field-plate. The other is the sensitivity difference between the UVIII and PMMA is large (~13), causing negligible influence on the foot layer PMMA. Dose tests for the footprint are undertaken with a dose range from 900 μC/cm^2 to 1500 μC/cm^2 for the PMMA (350K) and from 400 μC/cm^2 to 500 μC/cm^2 for the PMMA (100K), respectively.

As shown in Fig. 1a, after e-beam exposure, post exposure bake (PEB) is immediately done on a hot plate at 130 °C for 90 s, followed by a two-step developing process. Development of the exposed UVIII in Shipley CD 26 developer is first carried out for 60 s. In this step, the 10 nm Al layer is also removed by the alkali developer, creating a cleared area for the field-plate. In the second step, the bilayer of PMMA (350K)/PMMA (100K) is developed in O-xylene for 60 s, leaving a wide V-groove like profile in the foot part due to the difference of sensitivities between the two PMMA layers. Since O-xylene is not dissolved in water, after developing, it is cleared away by a stream of flowing de-ionized water. In both steps, a fixed developing temperature of 23 °C is used.

Reactive ion etching is undertaken to transfer the foot profile from the bilayer of PMMA into the SiNx layer, as shown in Fig. 1b. Metallized gates are formed by thermal heating evaporation of chromium (15 nm)/gold (300 nm) and the lift-off process is done in warm acetone (Fig. 1c).

The inspection of the resist profiles is carried out by a scanning electron microscope, (Zeiss Sigma-HD SEM). The lithography property of PMMA and UVIII, such as contrast and sensitivity is characterized by contrast curves using a Bruker stepper. The dissolution rates of PMMA and UVIII are also derived from the contrast curves. The RIE process is carried out by a Samco RIE-10NR etcher. The thermal heated evaporator, Kurt J. Lesker Nano 36 is used for the metallization process.

3. Results and discussion

3.1. Characterization of PMMA350K/PMMA100K/UVIII trilayer resists

To evaluate the trilayer resist, both contrasts and sensitivities are measured by contrast curves for UVIII, PMMA (MW 350K) and PMMA (MW 100K), which are presented in Fig. 2 for comparison, where the lines are just a guide to the eye. Table 1 concludes the contrasts and sensitivities of UVIII, PMMA (MW 350K) and PMMA (MW 100K) derived from the contrast curves in Fig. 2. Each

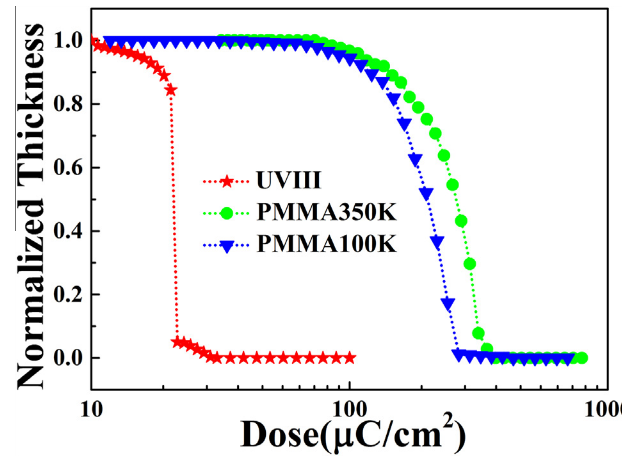

Fig. 2. Contrast curves of UVIII, PMMA100K and PMMA350K, respectively, measured by a Bruker stepper. The exposed UVIII is developed in alkali CD26 developer. Both PMMA (100K) and PMMA (350K) are developed by O-xylene solution.

Table 1
Characteristics of UVIII, PMMA100K, and PMMA350K resist, which are derived by the contrast curves.

Resist	Contrast	Sensitivity (μC/cm$^{2)}$	Actual dose (μC/cm$^{2)}$
CD26	10.6	22.8	40–50
PMMA100K	3.56	260	400–500
PMMA350K	3.43	340	900–1500

contrast is calculated by the average slope of the curve between two heights at 25% and 75% of the resist thickness, respectively. The sensitivity, also known as the clearing dose, is defined by the intercept of the straight line passing through the two points (25% and 75%) with the dose-axis.

In this work, the contrast curves, which carry the information of sensitivity and contrast of the resists, are used as a guide in designing the layer structure for achieving a large field-plate with a narrow foot. On one hand, the bilayer of PMMA, the top PMMA (100K) is slightly more sensitive than the bottom PMMA (350K), creating a wide V-groove like profile after lithography as demonstrated in Fig. 3. On the other hand, UVIII has much higher sensitivity than both PMMA350K and PMMA100K, it generates a broad open area for the field-plate as presented in Fig. 3 by a dose of 40–50 μC/cm^2. Such a small dose has negligible effect on the PMMA layer

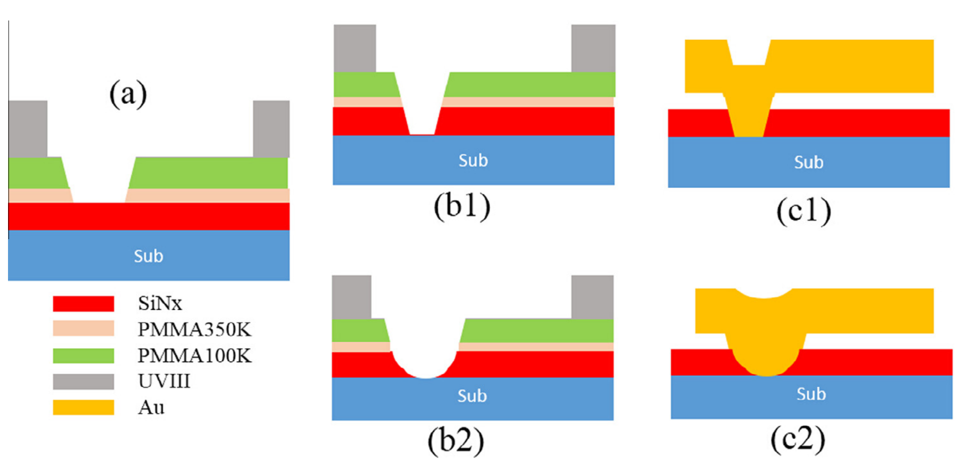

Fig. 1. Schematic diagrams for the process flow and the SiNx/PMMA350K/PMMA100K/UVIII layer stack for air spaced field-plate (ASFP) gates on substrate. (a) T shape profile after electron beam exposure and a two-step development process; (b1) tapering shape profile in the resist/SiNx layer after RIE etch; (b2) curvy shape profile in the resist/SiNx layer after RIE etch; (c1) tapering shape foot of ASFP gates after metallization and lift off process; (c2) curvy shape foot of ASFP gates after metallization and lift off process. The air-space underneath the field-plate should be kept very small for suppressing the peak-field existing in the conducting channel.